Exploration and optimization of substituted triazolothiadiazines and triazolopyridazines as PDE4 inhibitors

Amanda P. Skoumbourdis [a], Christopher A. LeClair [a], Eduard Stefan [b,†], Adrian G. Turjanski [c], William Maguire [a], Steven A. Titus [a], Ruili Huang [a], Douglas S. Auld [a], James Inglese [a], Christopher P. Austin [a], Stephen W. Michnick [b], Menghang Xia [a], Craig J. Thomas [a,*]

[a] NIH Chemical Genomics Center, National Human Genome Research Institute, NIH 9800 Medical Center Drive, MSC 3370 Bethesda, MD 20892-3370, USA
[b] Département de Biochimie, Université de Montréal, C.P. 6128, Succursale Centre-Ville, Montréal, QC, Canada H3C 3J7
[c] Oral and Pharyngeal Cancer Branch, National Institute of Dental and Craniofacial Research, NIH Bethesda, MD 20892-3370, USA

ARTICLE INFO

ABSTRACT

An expansion of structure–activity studies on a series of substituted 7H-[1,2,4]triazolo[3,4-b][1,3,4]thiadiazine PDE4 inhibitors and the introduction of a related [1,2,4]triazolo[4,3-b]pyridazine based inhibitor of PDE4 is presented. The development of SAR included strategic incorporation of known substituents on the critical catechol diether moiety of the 6-phenyl appendage on each heterocyclic core. From these studies, (R)-3-(2,5-dimethoxyphenyl)-6-(4-methoxy-3-(tetrahydrofuran-3-yloxy)phenyl)-7H-[1,2,4]triazolo[3,4-b][1,3,4]thiadiazine (**10**) and (R)-3-(2,5-dimethoxyphenyl)-6-(4-methoxy-3-(tetrahydrofuran-3-yloxy)phenyl)-[1,2,4]triazolo[4,3-b]pyridazine (**18**) were identified as highly potent PDE4A inhibitors. Each of these analogues was submitted across a panel of 21 PDE family members and was shown to be highly selective for PDE4 isoforms (PDE4A, PDE4B, PDE4C, PDE4D). Both **10** and **18** were then evaluated in divergent cell-based assays to assess their relevant use as probes of PDE4 activity. Finally, docking studies with selective ligands (including **10** and **18**) were undertaken to better understand this chemotypes ability to bind and inhibit PDE4 selectively.

© 2009 Published by Elsevier Ltd.

The second messenger cyclic 3,5-adenosine monophosphate (cAMP) is a key regulator of numerous signaling cascades.[1,2] As such, the production of cAMP by adenylate cyclase (AC) and the degradation of cAMP by phosphodiesterases (PDEs) are highly regulated. There are 11 primary families of PDEs (designated PDE1–PDE11) expressed throughout the human body, with several families having multiple isoforms. Much effort has been devoted to understanding the physiological role of each PDE isoform, and the pharmacological inhibition of select PDE isoforms has proven therapeutically beneficial for several indications.[2–4] The PDE4 family is comprised of 4 primary gene products (PDE4A, PDE4B, PDE4C, PDE4D) and is highly expressed in neutrophils and monocytes, CNS tissue and smooth muscles of the lung.[2–4] Not surprisingly, the clinical utility of PDE4 inhibitors has focused on asthma, chronic obstructive pulmonary disease (COPD), memory enhancement and as a general modulator of inflammation.[4]

At present, there are numerous chemotypes known to inhibit PDE4 and several of these inhibitors are currently being evaluated in clinical settings.[5] Reported molecules include rolipram (**1**), roflumilast (**2**) and cilomilast (**3**). It is notable that each of these small molecules contains a common catechol diether motif. Crystallographic studies of PDE4 bound to several of these derivatives have shown the catechol diether forming a key hydrogen bond with a conserved glutamine residue (Gln443 in PDE4B and Gln369 in PDE4D).[4,6,7] The choice of alkyl, cycloalkyl and heterocyclic ether moieties is presumably driven by improvements to the potency of each molecule and selected DMPK properties. It is noteworthy that methoxy, cyclopentyloxy, cyclopropylmethoxy and 2-difluoromethoxy are repeatedly incorporated into known PDE4 inhibitor scaffolds. Another common ether substituent, an O-3-tetrahydrofuranyl such as in **4**, is found in numerous published and patented chemotypes.[8–10] The frequency with which these moieties are incorporated on small molecules intended to down-regulate PDE4 is compelling. However, there are few reports that directly compare these substituents on the same core chemotype to gain an appreciation of each moieties potential and limitations.

Recently, we introduced a series of substituted 7H-[1,2,4]triazolo[3,4-b][1,3,4]thiadiazines as potent PDE4 inhibitors including **5**.[11] Our initial 77 member matrix library revealed that the 3,4-catechol diether motif on the 6-phenyl appendage on the triazolothiadiazine ring system played a key role in defining this chemo-
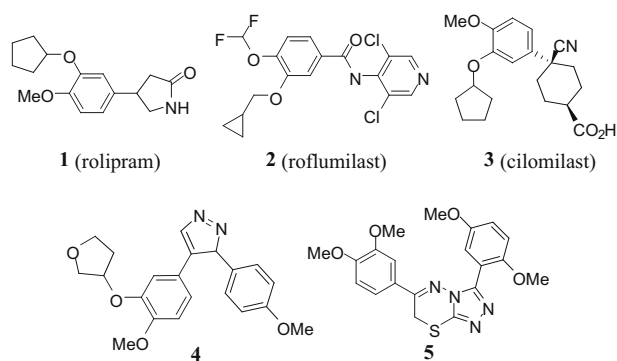
Figure 1. Structures of several known PDE4 inhibitors.

type's pharmacophore. Here, we systematically incorporate the methoxy, cyclopentyloxy, cyclopropylmethoxy, 2-difluoromethoxy and O-3-tetrahydrofuranyl moieties onto the 6-phenyl-triazolothiadiazine core in an attempt to improve potency, but also better understand these frequently utilized groups. The DMPK profiles of a representative triazolothiadiazine showed low microsomal stability (rat) [high intrinsic clearance (Clint >300 μL/min/mg protein) and short half-life ($t_{1/2} \sim 3$ min)]. The removal/alteration of aromatic methoxy groups has been shown to positively affect microsomal stability in several instances given the propensity for demethylation and glucuronidation of this functional group. We were further interested in transposing the substitution patterns found on the triazolothiadiazine ring to the related triazolopyridazine ring system in order to remove the lone sulfur atom and eliminate S-oxidation as an additional mechanism of metabolism and clearance (Fig. 1).

The synthesis of substituted 7H-[1,2,4]triazolo[3,4-b][1,3,4]thiadiazines was accomplished via previously reported methods (for full synthetic details associated with the synthesis of substituted 7H-[1,2,4]triazolo[3,4-b][1,3,4]thiadiazines see the Supporting information).[11] The key condensation reaction between appropriately substituted 2-bromo-1-phenylethanone (ultimately the phenyl ring at the C6 position of the heterocycle) and appropriately substituted 4-amino-3-phenyl-1H-1,2,4-triazole-5(4H)-thione (ultimately the phenyl ring at the C3 position of the heterocycle) was accomplished in ethanol at elevated temperatures. Utilizing the known SAR from our previously reported matrix library, we opted to maintain the 2,5-dimethoxy substitution pattern on the 3-phenyl appendage on the heterocyclic core. To incorporate the

cyclopentyloxy, cyclopropylmethoxy, 2-difluoromethoxy and O-3-tetrahydrofuranyl moieties on to the 2-bromo-1-phenylethanone precursor, we relied upon 1-(3-hydroxy-4-methoxyphenyl)ethanone as an orthogonally protected starting reagent. For the cyclopentyloxy and cyclopropylmethoxy substituents, we utilized a nucleophilic displacement of the corresponding alkyl bromides to ultimately provide the substitution pattern found in derivatives **6** and **7** (Table 1). Reaction of 1-(3-(cyclopentyloxy)-4-methoxyphenyl)ethanone with dodecane-1-thiol in sodium methoxide/DMF at 100 °C provided demethylation in a mild manner.[12] Treatment of the resulting 1-(3-(cyclopentyloxy)-4-hydroxyphenyl)ethanone with sodium 2-chloro-2,2-difluoroacetate in DMF at 100 °C afforded the incorporation of the 2-difluoromethoxy functionality on the C4 position of the catachol moiety (found in derivative **8**).[13] Mitsonobu conditions were utilized to condense tetrahydrofuran-3-ol (both racemic and R) with 1-(3-hydroxy-4-methoxyphenyl)ethanone to provide analogues **9** and **10**.

The synthesis of [1,2,4]triazolo[4,3-b]pyridazines was based upon the precedented works of Tišler and coworkers, Greenblatt and coworkers and Street and coworkers.[14–16] The general method is outlined in Scheme 1 and begins with the coupling of commercially available 2,5-dimethoxybenzoic acid (**11**) and 3-chloro-6-hydrazinylpyridazine (**12**) to provide N'-(6-chloropyridazin-3-yl)-2,5-dimethoxybenzohydrazide (**13**) in good yields. Direct treatment of **13** with POCl₃ at elevated temperature afforded the cyclization to core [1,2,4]triazolo[4,3-b]pyridazine ring system (analogue **14**) and provided a common analogue for entry into the convergent syntheses of multiple products via end-stage Suzuki–Miyaura couplings. Here, we were primarily interested in examining the biochemical viability of this alternate heterocycle and limited our explorations to the appropriately substituted O-3-tetrahydrofuranyl derivatives. Boronic acids **15** and **16** were synthesized independently utilizing the aforementioned Mitsonobu protocols and displacement of an aryl bromide with boronic acid. Following purification of **15** and **16**, standard Suzuki–Miyaura conditions with microwave irradiation produced the appropriately substituted [1,2,4]triazolo[4,3-b]pyridazines **17** and **18** in good yields.

PDE4A inhibition profile. With several new analogues now in hand, we evaluated their inhibitory potency against PDE4A via a previously reported, purified enzyme fluorescence polarization assay (IMAP; Molecular Devices, CA).[11] The results for the newly synthesized 7H-[1,2,4]triazolo[3,4-b][1,3,4]thiadiazines **5–10** and the novel [1,2,4]triazolo[4,3-b]pyridazines **17** and **18** are shown in Table 1. For 7H-[1,2,4]triazolo[3,4-b][1,3,4]thiadiazines **5–10**, each

Table 1
PDE4A inhibition by compounds **5–10**, **17** and **18**.[*]

	Analogue #	R^1	R^2	PDE4A IC₅₀ (nM)
5-10	**5**	−OCH₃	−OCH3	6.7 ± 0.4
	6	−OCypent	−OCH3	13 ± 0.8
	7	−OCH2Cyprop	−OCH3	6.1 ± 0.9
	8	−OCH2Cyprop	−OCHF₂	11 ± 0.7
17, 18	**9**	−O(3-THF)[rac]	−OCH3	3.4 ± 0.4
	10	−O(3-THF)[R]	−OCH3	3.0 ± 0.2
	17	−O(3-THF)[S]	−OCH3	7.3 ± 3.8
	18	−O(3-THF)[R]	−OCH3	1.5 ± 0.7

[*] Data represents the results from three separate experiments. Definitions: OCH₃ = methoxy, OCypent = cyclopentyloxy, OCH₂Cyprop = cyclopropylmethoxy, OCHF₂ = 2-difluoromethoxy, O(3-THF) = O-3-tetrahydrofuranyl [racemic, RorS enantiomers].
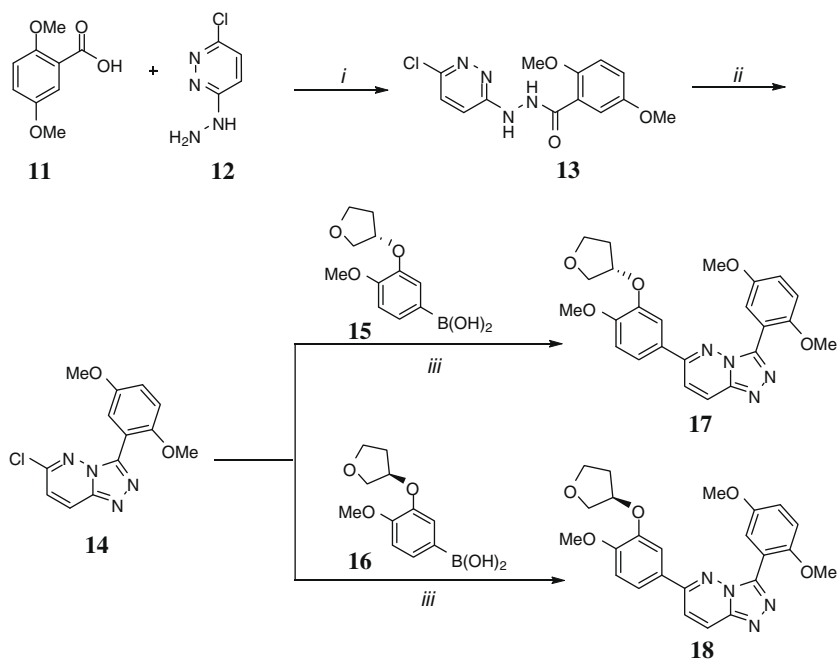
Scheme 1. Reagents and conditions: (i) CDI, DMF, rt 2 h; (ii) POCl3, 105 oC, 2 h; (iii) 15 or 16, Pd(PPh3)4, 2 M aq. Na$_2$CO$_3$, DME, μwave, 90 °C 30 min.

substitution pattern yielded a molecule with potency in the low nanomolar range. The enantiomerically pure O-(3-THF)[R] substitution of **10** showed the best potency with an IC$_{50}$ value of 3.0 nM. As a result, the enantiomerically pure O-(3-THF)[R] and O-(3-THF)[S] substitutions were incorporated onto the [1,2,4]triazolo[4,3-b]pyridazine core structure and the resulting constructs were found to have excellent potencies for PDE4A inhibition (IC$_{50}$ value of 7.3 ± 3.8 nM for **17** and 1.5 ± 0.7 nM for **18**). Several analogues were also explored with varying substitutions on the phenyl ring attached to the C3 position of the 1,2,4-triazole ring system. Substitutions included methoxy, fluoro, chloro and trifluoromethyl groups on the ortho, meta and para positions of the phenyl ring (for synthetic details and characterization of these analogues see Supporting Information section). Analysis of these analogues confirmed that various substitutions at one of the ortho positions were necessary to maintain potent PDE4A inhibition (see Supporting information). Additional substitutions have been shown to be tolerated without effect on the inhibition of PDE4A.

Selectivity panel of PDE isoforms. Having arrived at several compounds with good potency profiles and divergent core heterocycles, it was of interest to confirm the selectivity of these agents against a panel of PDE isoforms. BPS Bioscience (San Diego, CA)[17] has available a panel of 21 PDE isoforms from all 11 primary PDE families except PDE6 available for activity profiling. We submitted **5**, **10**, **18** and **1** for analysis across this panel and the resulting IC$_{50}$ determinations are shown in Table 2.

It is apparent that both **10** and **18** represent novel inhibitors of five isoforms of PDE4 with sub-nanomolar potencies found for PDE4A1A. The modest activities found for PDE3B and PDE10A1 represent a sizeable enough difference in potency that cellular phenotypes will not be complicated by dual activities. Interestingly, PDE10 is considered to be an important modulator of cGMP regulation in the brain. To date few reports of potent and selective PDE10 inhibitors have surfaced. Analogues **10** and **18** may represent good starting points for optimizing novel compounds as potent inhibitors of PDE10.

The identification of novel enzyme inhibitors via screening in purified enzyme assays provides an important means for the identification of small molecules with a known mechanism of action.
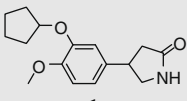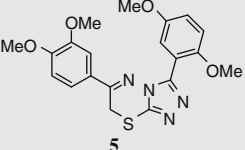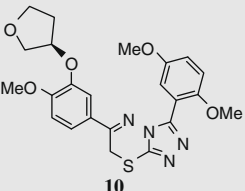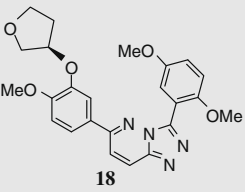
However, not all active small molecules found in such screens find utility in cell-based assays for a myriad of reasons. To evaluate whether the substantial *in vitro* inhibition of PDE4 by **10** and **18** could be replicated in living cells we pursued two divergent, cell-based assays of PDE4 activity.

Cyclic-nucleotide gated ion channel cell-based assay. The first cell-based analysis of PDE4 activity utilized a recently reported assay based on the coupling of a constitutively activated G-protein coupled receptor (the thyroid-stimulating hormone receptor (TSHR)) and cyclic-nucleotide gated (CNG) ion channel coexpressed in HEK293 cells.[18] The read-out for this assay is based on measurement of membrane electrical potential by a potential-sensitive fluorophore (ACTOne™ dye kit). Inhibitors of PDE4 will interfere with the native enzymatic conversion of cAMP to AMP resulting in increased intracellular levels of the cyclic nucleotide due to constitutive activity of the GPCR. In response to increased amounts of cAMP, the CNG ion channel opens resulting in membrane polarization. The dye reacts to this alteration in membrane polarity with an increase in fluorescence detectable by fluorescence spectroscopy of whole cells read on a fluorescence microtitre plate reader.

Compounds **5**, **10** and **18** were used in this analysis as along with the common PDE4 inhibitor **1**, and the results are shown in Figure 2. In this assay, **1** was noted to produce an effective response (EC$_{50}$) (registered as % activity) of 131.5 nM. In comparison, the triazolothiadiazine based inhibitors were found to be more potent in this cell-based assay with **5** and **10** registering an EC$_{50}$ value of 18.7 and 2.3 nM, respectively. The EC$_{50}$ of the lone triazolopyridazine **18** was 34.2 nM.

Protein-fragment complementation (PCA) cell-based assay. PCAs take advantage of the ability of well-engineered protein fragments to form a functional monomer with measurable enzymatic activity when brought into suitable proximity by interacting proteins to which the fragments are fused.[20,21] For our purposes, we utilized a previously described PCA based on the reporter enzyme *Renilla reniformis* luciferase (*Rluc*) N- and C terminal fragments of *Rluc* fused to the catalytic subunits (Cat) and inhibiting regulatory subunits (Reg) of protein kinase A (PKA).[19] The signaling cascades initiated by GPCR activation is mediated by cAMP production and activation of numerous protein kinases.[1,20] Negative regulation of

Table 2
PDE isoform selectivity data for **1**, **5**, **10** and **18**

	PDE isoform[*]	1 IC$_{50}$/% inh.	5 IC$_{50}$/%inh.	10 IC$_{50}$/%inh.	18 IC$_{50}$/%inh.
	PDE1A	Inactive	Inactive	36%	32%
	PDE 1B	Inactive	Inactive	52%	56%
	PDE1C	Inactive	26%	49%	74%
	PDE2A	Inactive	41%	68%	54%
	PDE3A	Inactive	1.7 μM	56%	54%
	PDE3B	Inactive	720 nM	4.6 μM	2.3 μM
	PDE4A1A	102 nM	12.9 nM	0.26 nM	0.6 nM
	PDE4B1	901 nM	48.2 nM	2.3 nM	4.1 nM
	PDE4B2	534 nM	37.2 nM	1.6 nM	2.9 nM
	PDE4C1	40%	452 nM	46 nM	106 nM
	PDE4D2	403 nM	49.2 nM	1.9 nM	2.1 nM
	PDE5A1	Inactive	60%	58%	51%
	PDE7A	Inactive	73%	48%	59%
	PDE7B	Inactive	33%	43%	35%
	PDE8A1	Inactive	57%	Inactive	Inactive
	PDE9A2	Inactive	Inactive	Inactive	Inactive
	PDE10A1	Inactive	823 nM	632 nM	388 nM
	PDE11A4	Inactive	Inactive	Inactive	Inactive

[*] Data generated by BPS Biosciences (CA) [http://www.bpsbioscience.com] and represents either the IC$_{50}$ value or the % inhibition at 10 μM of compound. Assays are based upon a fluorescence polarization assay using carboxyfluorescein (FAM)-cAMP as the binding probe.

these events is the sole domain of the phosphodiesterase class of enzymes.[2] One ubiquitous pathway is activated when cAMP triggers the disassociation of the PKA catalytic and regulatory subunits, which in turn, enables numerous signaling events. In the *Rluc* PCA PKA reporter, the regulatory subunit II beta cDNA is fused through a sequence coding for a flexible polypeptide linker of 10 amino acids (Gly.Gly.Gly.Gly.Ser)$_2$ to the N-terminal fragment (*Rluc* F[1])[amino acids 1–110 of *Rluc*] and the cDNA of the PKA catalytic
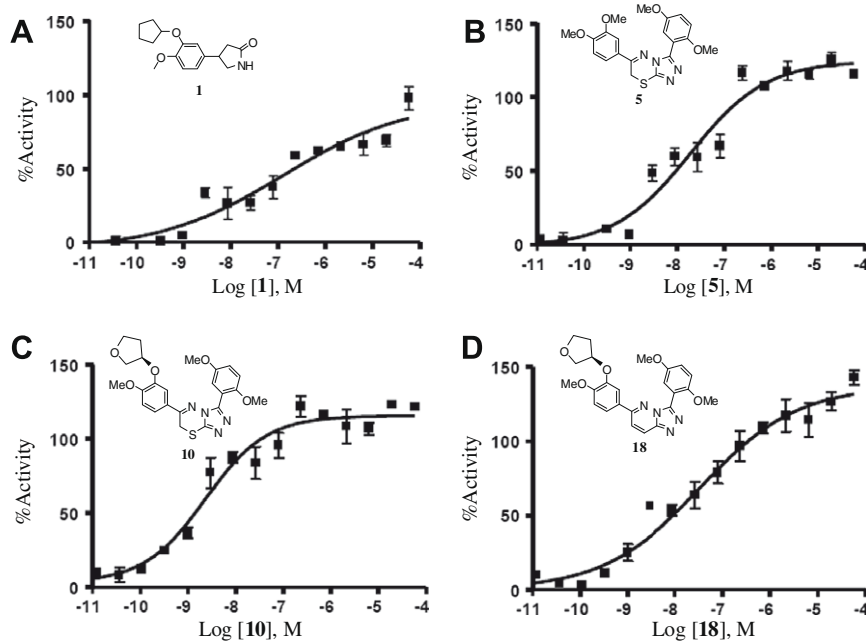
Figure 2. Cell-based analysis of novel PDE4 inhibitors. Effect of PDE4 inhibition by **1**, **5**, **10** and **18** in a cell-based cyclic nucleotide-gated cation channel biosensor assay. Specific EC$_{50}$ values are as follows: (A) EC$_{50}$ for **1** = 131.5 nM. (B) EC$_{50}$ for **5** = 18.7 nM. (C) EC$_{50}$ for **10** = 2.3 nM. (D) EC$_{50}$ for **18** = 34.2 nM. The data represents the results from four separate experiments.

subunit alpha is fused through the same flexible linker to the C-terminal fragment (*Rluc* F[2])[amino acids 111–311 of *Rluc*]. The resulting constructs Reg-F[1] and Cat-F[2] can reconstitute enzymatic activity of *Rluc* in the absence of cAMP. It has been recently demonstrated that this assay could be used to detect the effects of PDE4 inhibition on PKA activation downstream of basal β-2 adrenergic receptor (β2AR) activities.[19]

Here, we evaluated the effects of **1**, **10** and **18** in HEK293 cells stably expressing the β2AR and transiently transfected with the required PKA-*Rluc* fragments [Reg-F[1] and CatF-[2]]. It was confirmed that isoproterenol (**19**) activation of the β2AR is able to reduce luminescence (indicating dissociation of the *Rluc* biosensor complex and consequent activation of PKA catalytic activity) (Fig. 3A). Further, pretreatment with the selective β2AR inverse agonist ICI 118551 (**20**; decrease of basal β2AR activity) was capable of preventing the effects of **19** as was previously shown.[19] These important controls confirm that alterations of the luminescence signal are primarily mediated through the actions of the β2AR signaling to PKA. Further, the effect of **1** confirms the responsiveness of the assay to PDE4 inhibition. Treatment with **10** and **18** at 100 μM and 10 μM concentrations displayed marked loss of luminescence suggesting a β2AR mediated increase of cAMP due to inhibition of PDE4 (Fig. 3B). Next, we examined the real-time kinetics of PKA subunit dissociation by administering **10** at a 10 μM concentration. The shown real-time kinetics are normalized on the control experiment of administering **10** following pretreatment with 1 μM of the inverse β2AR agonist **20**. In four independent experiments, the presence of **10** reduced the luminescence of the cell-based system by 25% to 50% within 2 min of administration (Fig. 3C).

Docking of 10 at PDE4B. Given the potency, selectivity and cell-based PDE4 inhibition results for this chemotype, it was of interest to examine its binding modality to the PDE4 structure. The PDE classes of enzymes are comprised of an N-terminal domain, a catalytic domain and a C-terminal domain. Crystallographic analyses of several PDE isozymes have aided researchers in understanding the divergent activities and pharmacology of this class of proteins.[6,22] Importantly, structures of PDE4 have been reported in complex to AMP and several small molecule inhibitors.[23–27] Through these efforts it was shown that the three domains of PDE4 are coordinated through interactions with two metal cations (Zn^{2+} and Mg^{2+}).[7] The residues that coordinate these metals are highly conserved across the PDE family. Both the Zn^{2+} and Mg^{2+} play important roles in the catalytic mechanism of cAMP hydrolysis by coordinating the phosphate moiety. Other important insights include the recognition of a conserved glutamine residue (Q443 in

PDE4B) that serves as an important binding residue for the purine motif of cAMP and cGMP.

From the myriad of known PDE4 inhibitors, one common structural motif that continues to be exploited are catachol diether-based small molecules.[4] Indeed, the structure of **1** formed the basis for numerous catachol diether based inhibitors of PDE4 and the visualization of **1** bound to PDE4B provided the rational for its potent inhibition profile. From numerous crystallographic analyses and modeling efforts it is clear that the catachol diether based inhibitors bind to the catalytic domain of PDE4 through specific hydrogen bonds with the conserved glutamine residue. Our initial SAR explorations of triazolothiadiazine based PDE4 inhibitors confirmed that a 3,4-dimethoxy phenyl moiety linked to the C6 position of the 3,6-dihydro-2*H*-1,3,4-thiadiazine ring was a crucial substitution pattern for potent PDE4 inhibition.[11] Interestingly, the phenyl ring attached to the C3 position of the 1,2,4-triazole ring system was found to be more amendable to random substitutions without loss of function. This formed the basis for our supposition that these novel PDE4 inhibitors bind in a similar way to **1**.

To explore this hypothesis, we conducted docking simulations using the AutoDock software.[28] We first retrieved the three-dimensional coordinates for PDE4B from the Protein Data Bank (PDB ID: 1XMY). Protein and ligand structures were prepared in AutoDock[28] and previously reported PDE4-inhibitor complexes were taken into account when preparing the active site grid box. Flexibility was granted to the active site glutamine and the ligand(s). Following multiple docking simulations the most favorable binding conformations were extracted based upon calculated binding constants (reported as K_i values and found to be in the low nanomolar range for favorable docking orientations). The primary docking modality for **10** is shown in Fig. 4. Importantly, this docking orientation is consistent with the idea that the catachol diether forms an integral hydrogen bond with Q443 (right panel) and the aromatic moiety is clearly positioned between the conserved isoleucine (I410) and phenylalanine (F446). The remainder of the molecule is shown to extend into the catalytic domain in close proximity to both the Zn^{2+} and Mg^{2+} cations. Such an orientation would block the approach of cAMP to the catalytic domain and forms the basis for inhibiting PDE4. This docking orientation is consistent with the known SAR for this chemotype whereby the 3,4-dimethoxy phenyl moiety at the C6 position of the 3,6-dihydro-2*H*-1,3,4-thiadiazine ring is crucial for maintaining inhibition in the low nanomolar range whereas the opposite phenyl ring is more amendable to change without significant loss of potency. It also demonstrates that alterations of the core heterocycle from the general triazolothiadiazine structure to the triazolopyridazine structure will have
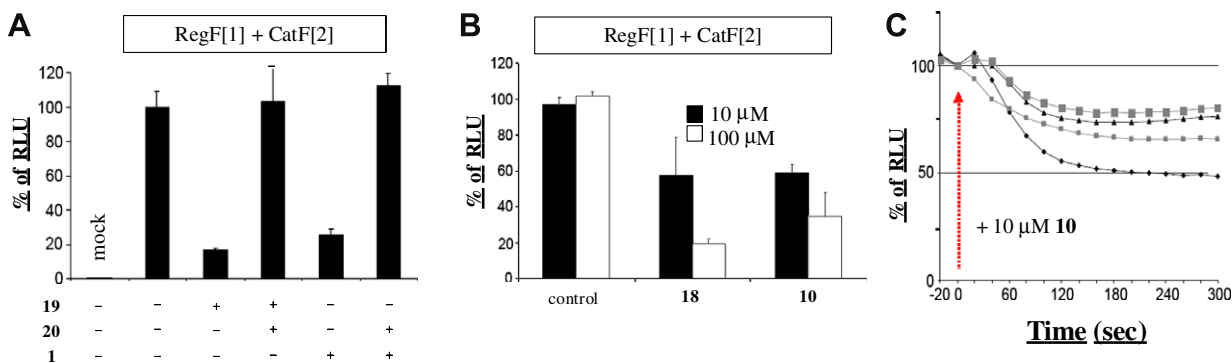
Figure 3. Effect of PDE inhibition on β2AR regulated PKA activities in cells. Bioluminescence (recorded in relative luminescence units or RLU) in A–C was detected from stable β2AR-HEK293 (see reference19) cells transiently transfected with the PKA reporter Reg-F[1]:Cat-F[2][2] (from three independent experiments). (**A**) Effect of combinations of pretreatment with the selective β2AR-antagonist **20** (1 μM) and treatment with **1** (100 μM; 30 min) or **19** (1 μM, 30 min) on the association of Reg-F[1]:Cat-F[2] (mean ± s.d. from independent triplicates). (**B**) Concentration dependent effect of **18**, **10** on the association of Reg-F[1]:Cat-F[2] (30 min, mean ± s.d. from independent triplicates). Percentage of PKA activation is normalized based upon **20** (1 μM) pretreated cells. (**C**) Real-time kinetics (normalized on the control experiment = pretreatment with 1 μM **20**) of Reg-F[1]:Cat-F[2] dissociation in response to **10** treatment (10 μM, four independent samples).
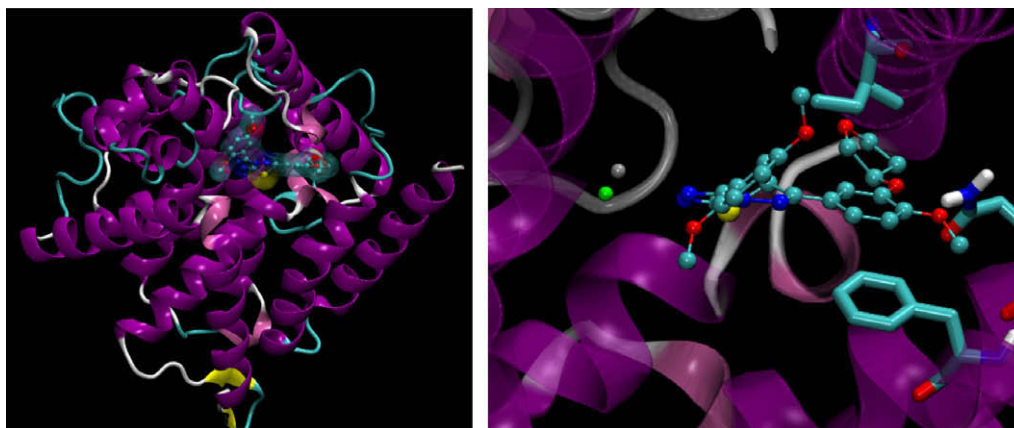
Figure 4. Model of PDE4B and docking of 10. The left panel details the entire PDE4B structure (N-terminal domain, a catalytic domain and a C-terminal domain) bound to **10**. The right panel shows the catalytic domain bound to **10** including interactions with conserved glutamine (Q443) isoleucine (I410) and phenylalanine (F446) and the Zn^{2+} (grey) and Mg^{2+} (green) cations.

limited affect on the inhibitory profile of these reagents. These docked structures may allow future SAR explorations to focus on improved pharmacokinetic and drug metabolism properties without compromising potency, efficacy and selectivity for this chemotype.

Numerous chemotypes exist for the potent, selective inhibition of PDE4. Here, we expand upon our discovery of substituted 6-(3,4-dialkoxyphenyl)-7H-[1,2,4]triazolo[3,4-b][1,3,4]thiadiazines and introduce 6-(3,4-dialkoxyphenyl)-[1,2,4]triazolo[4,3-b]pyridazines as novel inhibitors of PDE4. In this study, we examined the common structural substitutions found on other catachol diether based inhibitors of PDE4 and several of the resulting analogues are among the most potent inhibitors of this important cellular target. These include methoxy, cyclopentyloxy, cyclopropylmethoxy, 2-difluoromethoxy and O-3-tetrahydrofuranyl moieties. It was found that the chirally pure R-O-3-tetrahydrofuranyl substitution maintained the best potency in this study. Further, these reagents possess impressive selectivity for PDE4 versus other PDE family members. However, these chemotypes, like others, do not posses subtype selectivity across PDE4 isozymes.[4]

Our initial analysis of the compounds and their activity was based upon an in vitro analysis using purified PDE4 protein. It is critical to examine chemical probes discovered via purified-protein assays within cell-based contexts to confirm activity and establish that they are relevant for cell-based experimentation. Here, we examine selected analogues (**5**, **10** and **18**) in two different cell-based assays. One assay is based upon the ability of PDE4 to reduce cAMP levels in a CNG cell line while the other utilizes a PCA reporter for PKA activity. Both analyses demonstrated the utility of these novel reagents as cell-based chemical probes of PDE4 activity.

Finally, with the myriad of structural data surrounding PDE4 and PDE4 complexes with selected inhibitors, it was important to explore the binding modality of these compounds. Docking studies demonstrated that these agents utilize the conserved binding mode whereby the catachol diether functionality forms a strong interaction with a conserved glutamine residue. This docking orientation further provides a roadmap for additional SAR around the seemingly modifiable phenyl ring attached to the 1,2,4-triazole moiety of the core heterocycle. This key aspect of these reagents may be of importance during attempts to modify ADME properties of these compounds without altering the affinity or selectivity for PDE4.

PDE4 inhibitors are highly sought after as probes of selected cell signalling pathways and as potential therapeutics in diverse areas including memory enhancement and COPD. Here, we expand on

the potential of substituted triazolothiadiazines and introduce triazolopyridazines as potent and selective inhibitors of this important cellular target. Not only are selected analogues of this novel chemotype capable of down-regulating purified isozymes of PDE4, but they maintain excellent cell-based activity as well. Their binding modality is predicted to mimic known catachol diether based inhibitors of PDE4. Importantly, both computational and structure activity studies suggest that the phenyl ring at the C3 position of the 1,2,4-triazole ring system could be modified providing a mechanism for advanced SAR considerations.

Acknowledgments

Supplementary data

Experimental methods for the cyclic nucleotide-gated cation channel assay, protein-fragmentation complementation assays and molecular docking and the full synthetic procedures and characterization of reported compounds are detailed. This material is available free of charge via the Internet. Supplementary data associated with this article can be found, in the online version, at doi:10.1016/j.bmcl.2009.01.057.

References and notes

1. Beavo, J. A.; Brunton, L. L. Nat. Rev. Mol. Cell. Biol. **2002**, 3, 710.
2. Bender, A. T.; Beavo, J. A. Pharmacol. Rev. **2006**, 58, 488.
3. McKenna, J. M.; Muller, G. W. In Cyclic Nucleotide Phosphodiesterases in Health and Disease; Beavo, J. A., Francis, S. H., Houslay, M. D., Eds.; CRC Press, 2006; p 667.
4. Zhang, K. Y. J.; Ibrahim, P. N.; Gillette, S.; Bollag, G. Expert Opin. Ther. Targets **2005**, 9, 1283.
5. Huang, Z.; Ducharme, Y.; Macdonald, D.; Robichaud, A. Curr. Opin. Chem. Biol. **2001**, 5, 432.
6. Xu, R. X.; Rocque, W. J.; Lambert, M. H.; Vanderwall, D. E.; Luther, M. A.; Notle, R. T. J. Mol. Biol. **2004**, 337, 355.
7. Card, G. L.; England, B. P.; Suzuki, Y.; Fong, D.; Powell, B.; Lee, B.; Luu, C.; Tabrizizad, M.; Gillette, S.; Ibrahim, P. N.; Artis, D. R.; Bollag, G.; Milburn, M. V.; Kim, S.-H.; Schlessinger, J.; Zhang, K. Y. J. Structure **2004**, 12, 2233.
8. Dunn, R. F.; Kuester, E. M.; Conticello, R. D.; Hopper, A. T. WO 2007123953, 2007; PCT Int. Appl.

9. Napoletano, M.; Norcini, G.; Pellacini, F.; Marchini, F.; Morazzoni, G.; Ferlenga, P.; Pradella, L. *Bioorg. Med. Chem. Lett.* **2000**, *10*, 2235.
10. Andrés, J. I.; Alonso, J. M.; Diaz, A.; Fernández, J.; Iturrino, L.; Martinez, P.; Matesanz, E.; Freyne, E. J.; Deroose, F.; Boeckx, G.; Petit, D.; Diels, G.; Megens, A.; Somers, M.; Van Wauwe, J.; Stoppie, P.; Cools, M.; De Clerck, F.; Peeters, D.; de Chaffoy, D. *Bioorg. Med. Chem. Lett.* **2002**, *12*, 653.
11. Skoumbourdis, A. P.; Huang, R.; Southall, N.; Leister, W.; Guo, V.; Cho, M.-H.; Inglese, J.; Nirenberg, M.; Austin, C. P.; Xia, M.; Thomas, C. J. *Bioorg. Med. Chem. Lett.* **2008**, *18*, 1297.
12. Katoh, T.; Awasaguchi, K.-i.; Mori, D.; Kimura, H.; Kajimoto, T.; Node, M. *Synlett* **2005**, *19*, 2919.
13. Hall, A.; Brown, S. H.; Chessell, I. P.; Chowdhury, A.; Clayton, N. M.; Coleman, T.; Giblin, G. M. P.; Hammond, B.; Healy, M. P.; Johnson, M. R.; Metcalf, A.; Michel, A. D.; Naylor, A.; Novelli, R.; Spalding, D. J.; Sweeting, J.; Winyard, L. *Bioorg. Med. Chem. Lett.* **2007**, *17*, 916.
14. Pollak, A.; Tišler, M. *Tetrahedron* **1966**, *22*, 2073.
15. Albright, J. D.; Moran, D. B.; Wright, W. B., Jr.; Collins, J. B.; Beer, B.; Lippa, A. S.; Greenblatt, E. N. *J. Med. Chem.* **1981**, *24*, 592.
16. Carling, R. W.; Madin, A.; Guiblin, A.; Russell, M. G. N.; Moore, K. W.; Mitchinson, A.; Sohal, B.; Pike, A.; Cook, S. M.; Ragan, I. C.; McKernan, R. M.; Quirk, K.; Ferris, P.; Marshall, G.; Thompson, S. A.; Wafford, K. A.; Dawson, G. R.; Atack, J. R.; Harrison, T.; Castro, J. L.; Street, L. *J. Med. Chem.* **2005**, *48*, 7089.
17. BPS Bioscience Inc.; 11526 Sorrento Valley Rd. Ste. A2; San Diego, CA 92121. www.bpsbioscience.com.
18. Titus, S. A.; Xiao, L.; Southall, N.; Lu, J.; Inglese, J.; Brasch, M.; Austin, C. P.; Zheng, W. *J. Biomol. Screen.* **2008**, *13*, 609.
19. Stefan, E.; Aquin, S.; Berger, N.; Landry, C. R.; Nyfeler, B.; Bouvier, M.; Michnick, S. W. *Proc. Natl. Acad. Sci. U.S.A.* **2007**, *104*, 16916.
20. Michnick, S. W.; Ear, P. H.; Manderson, E. N.; Remy, I.; Stefan, E. *Nat. Rev. Drug Discov.* **2007**, *6*, 569.
21. Remy, I.; Michnick, S. W. *BioTechniques* **2007**, *42*, 137.
22. Xu, R. X.; Hassell, A. M.; Vanderwall, D.; Lambert, M. H.; Holmes, W. D.; Luther, M. A.; Rocque, W. J.; Milburn, M. V.; Zhao, Y.; Ke, H.; Nolte, R. T. *Science* **2000**, *288*, 1822.
23. Lee, M. E.; Markowitz, J.; Lee, J.-O.; Lee, H. *FEBS Lett.* **2002**, *530*, 53.
24. Huai, Q.; Colicelli, J.; Ke, H. *Biochemistry* **2003**, *42*, 13220.
25. Huai, Q.; Wang, H.; Sun, Y.; Kim, H.-Y.; Liu, Y.; Ke, H. *Structure* **2003**, *11*, 865.
26. Huai, Q.; Wang, H.; Zhang, W.; Colman, R. W.; Robinson, H.; Ke, H. *Proc. Nat. Acad. Sci. U.S.A.* **2004**, *101*, 9624.
27. Huai, Q.; Liu, Y.; Francis, S. H.; Corbin, J. D.; Ke, H. *J. Biol. Chem.* **2004**, *279*, 13095.
28. Morris, G. M.; Goodsell, D. S.; Halliday, R. S.; Huey, R.; Hart, W. E. *J. Comput. Chem.* **1998**, *19*, 1639.